



Article scientifique

Article

2006

Published version

Open Access

This is the published version of the publication, made available in accordance with the publisher's policy.

Regional brain development in serial magnetic resonance imaging of low-risk preterm infants

Mewes, Andrea U J; Hüppi, Petra Susan; Als, Heidelise; Rybicki, Frank J; Inder, Terrie E; McAnulty, Gloria B; Mulkern, Robert V; Robertson, Richard L; Rivkin, Michael J; Warfield, Simon K

How to cite

MEWES, Andrea U J et al. Regional brain development in serial magnetic resonance imaging of low-risk preterm infants. In: Pediatrics, 2006, vol. 118, n° 1, p. 23–33. doi: 10.1542/peds.2005-2675

This publication URL: <https://archive-ouverte.unige.ch/unige:72877>

Publication DOI: [10.1542/peds.2005-2675](https://doi.org/10.1542/peds.2005-2675)

Regional Brain Development in Serial Magnetic Resonance Imaging of Low-Risk Preterm Infants

Andrea U. J. Mewes, MD^a, Petra S. Hüppi, MD^b, Heidelise Als, PhD^c, Frank J. Rybicki, MD, PhD^a, Terrie E. Inder, MD^d, Gloria B. McAnulty, PhD^c, Robert V. Mulkern, PhD^e, Richard L. Robertson, MD^e, Michael J. Rivkin, MD^f, Simon K. Warfield, PhD^{a,e}

^aDepartment of Radiology, Brigham and Women's Hospital, Harvard Medical School, Boston, Massachusetts; ^bChild Development Unit, Department of Pediatrics, University Children's Hospital, Geneva, Switzerland; Departments of ^cPsychiatry, ^eRadiology, and ^fNeurology, Children's Hospital, Harvard Medical School, Boston, Massachusetts; ^dDepartment of Pediatrics, Washington University, St Louis, Missouri

The authors have indicated they have no financial relationships relevant to this article to disclose.

ABSTRACT

OBJECTIVE. MRI studies have shown that preterm infants with brain injury have altered brain tissue volumes. Investigation of preterm infants without brain injury offers the opportunity to define the influence of early birth on brain development and provide normative data to assess effects of adverse conditions on the preterm brain. In this study, we investigated serial MRI of low-risk preterm infants with the aim to identify regions of altered brain development.

METHODS. Twenty-three preterm infants appropriate for gestational age without magnetic resonance–visible brain injury underwent MRI twice at 32 and at 42 weeks' postmenstrual age. Fifteen term infants were scanned 2 weeks after birth. Brain tissue classification and parcellation were conducted to allow comparison of regional brain tissue volumes. Longitudinal brain growth was assessed from preterm infants' serial scans.

RESULTS. At 42 weeks' postmenstrual age, gray matter volumes were not different between preterm and term infants. Myelinated white matter was decreased, as were unmyelinated white matter volumes in the region including the central gyri. The gray matter proportion of the brain parenchyma constituted 30% and 37% at 32 and 42 weeks' postmenstrual age, respectively.

CONCLUSIONS. This MRI study of preterm infants appropriate for gestational age and without brain injury establishes the influence of early birth on brain development. No decreased cortical gray matter volumes were found, which is in contrast to findings in preterm infants with brain injury. Moderately decreased white matter volumes suggest an adverse influence of early birth on white matter development. We identified a sharp increase in cortical gray matter volume in preterm infants' serial data, which may correspond to a critical period for cortical development.

www.pediatrics.org/cgi/doi/10.1542/peds.2005-2675

doi:10.1542/peds.2005-2675

Key Words

magnetic resonance imaging, preterm infants, regional brain development, parcellation, segmentation

Abbreviations

UMWM—unmyelinated white matter
MWM—myelinated white matter
PMA—postmenstrual age
AGA—appropriate for gestational age
ICV—intracranial volume
MR—magnetic resonance
SPGR—spoiled gradient recalled
CSF—cerebrospinal fluid
CGM—cortical gray matter
SGM—subcortical gray matter
CPAR—cerebral parenchyma
STAPLE—Simultaneous Truth and Performance Level Estimation
ANCOVA—analysis of covariance

Accepted for publication Feb 13, 2006

Address correspondence to Andrea U. J. Mewes, MD, Department of Radiology, Brigham and Women's Hospital, 75 Francis St, Boston, MA 02115. E-mail: mewes@bwh.harvard.edu

PEDIATRICS (ISSN Numbers: Print, 0031-4005; Online, 1098-4275). Copyright © 2006 by the American Academy of Pediatrics

PRETERM INFANTS ARE at risk for adverse neurodevelopmental outcome and functional disabilities because of increased vulnerability of the brain before and after premature birth.^{1,2} Brain injury, seen as white and gray matter signal abnormalities and enlarged ventricles, can be clinically recognized with MRI.^{3,4} Providing high-resolution images of the living subject, this modality has also become a major tool for preterm brain research. MRI research has provided insight into the morphology and etiology of white matter injury and gray matter abnormalities.^{3,4} MRI-visible brain injury has been linked to hypoxic-ischemic incidences,⁵ and the severity of the injury has been shown to depend on epidemiologic factors, such as perinatal infection^{6,7} and hypotension with use of inotrope medication.⁸

Recently, image postprocessing including segmentation⁹ and parcellation¹⁰ has contributed to the understanding of the relationship between brain injury and quantitative morphologic changes of the major brain tissue compartments. Several conditions, such as periventricular leukomalacia and fetal growth restriction, have been found to affect white and gray matter development in preterm infants when compared with healthy term infants.^{10–15} Whereas most investigations compare total brain tissue volumes, studies assessing regional changes are few in number.^{10,16}

Investigations in preterm infants also offer the opportunity for the study of longitudinal brain development. In this context, an important indicator of brain development is the process of myelination. Early myelination is seen in preterm MRI as altered signal intensity, for example, high signal intensity on T1-weighted images in localized regions in the internal capsule and brainstem.¹⁷ The segmentation approach used in this study is based on MRI signal intensity contrast between brain tissues. This technique enabled the segmentation of 2 different tissue classes for unmyelinated (UMWM) and myelinated white matter (MWM).¹⁸

Infants who are born before 28 weeks' postmenstrual age (PMA), whose birth weight is <1000 g, or who suffer from fetal growth restriction seem at higher risk for brain injury. However, the majority of preterm infants are of moderate gestational age (>28 weeks' PMA) and moderate birth weight (>1500 g).^{19,20} Their risk for brain injury is recognized as low.^{21,22} However, research on these low-risk preterm infants' brain development is still very scarce. The limited existing studies report moderate developmental delay.^{23,24}

The aim of this study was to investigate by MRI the brain's appearance in a group of preterm infants born at 28 to 33 weeks' PMA, appropriate in growth for gestational age (AGA) at birth and without known risk factors for altered brain development. Preterm infants were scanned at 42 weeks' PMA, and the scans were compared with age-equivalent healthy term infants' scans. Postprocessing of the MRI acquisitions included segmen-

tation of brain tissues into 5 gray and white matter compartments and parcellation of the intracranial cavity (ICV)²⁵ to identify regional differences in brain tissue volumes. In addition, an early scan was acquired for each preterm infant soon after birth. This provided the opportunity to describe longitudinal brain development during the third trimester outside the womb. It was the aim of this study to define changes in the tissue composition of the brain and to investigate whether growth occurs at different rates in different regions.

METHODS

Subjects

Forty-three infants were included in the study; 26 (20 preterm and 6 term infants) born at the Brigham and Women's Hospital (Boston, MA) and part of a larger study²⁶; 8 preterm infants born at the Children's Hospital, (Geneva, Switzerland); and 9 term infants born at the Royal Women's Hospital (Melbourne, Australia). The gestational age of the infant at birth was estimated by mother's last menstrual period and early ultrasound. Infant age at the time of the scans is given as PMA, which is defined as gestational age plus the time elapsed since birth.²⁷

Preterm infants' selection criteria included gestational age at birth 28 to 33 weeks' PMA, 5-minute Apgar score ≥ 7 ; AGA for weight and head circumference at birth (>10th percentile for both); normal cranial ultrasound and baseline MRI; and <72 hours of mechanical ventilation and vasopressor medication. Exclusion criteria were congenital and chromosomal abnormalities, congenital and acquired infections, prenatal brain lesions (eg, cysts and infarctions), and neonatal seizures. Parents' selection criteria included absence of major medical and psychiatric illness, long-term medication treatment (eg, insulin, steroids, antidepressants, and anticonvulsants), and absence of a history of substance abuse, including tobacco and alcohol. Written, informed consent was obtained from all of the parents before enrollment into the study. Identical imaging study protocols were used across institutions after obtaining permission from each of the institutions review boards for research with human subjects.

MRI Acquisitions

Preterm infants were scanned at a 1.5-T magnetic resonance (MR) system (General Electric Signa, Milwaukee, WI, or 1.5 T Marconi Philipps Medical Systems, Andover, MA) after birth as soon as they were judged to be in stable condition. The mean PMA for the preterm infants' first scan was 33.3 ± 1.6 weeks acquired at 13 ± 6 days after birth. Scanning was repeated at 41.7 ± 1.7 weeks' PMA. Term infants were scanned at 41.7 ± 0.7 weeks' PMA. High-resolution ($0.7 \times 0.7 \times 1.5$ -mm coronal slices) T1-weighted three-dimensional Fourier

transform spoiled gradient recalled (SPGR) images were obtained (18-cm field of view, 1.5-mm contiguous slice thickness, repetition and echo times of 40 ms and 4 ms, matrix 256×256 , flip angle = 20°) requiring a scan time of 20 minutes. T2-weighted and proton density-weighted images were acquired using a dual echo fast spin echo sequence (echo train length: 8; 3-mm skip interleave; 2 acquisitions; repetition time: 4000; echo times: 160 and 80 ms; matrix: 256×256 ; field of view: 18 cm; number of excitations: 1; coronal slices: $0.7 \times 0.7 \times 3$ mm; scan time: 6.4 minutes). Before scanning, infants were fed, wrapped securely in warm blankets, outfitted with ear protection, and placed into the scanner on a vacuum pillow.

A neonatologist and/or NICU staff nurse responsible for the infants' transfer to the MR scanner also stayed with them in the scanner room during scanning to monitor their electrocardiography and pulse oximetry. All of the scans were performed without sedation. Five scans were excluded from the study, because motion artifacts were judged to interfere significantly with image post-processing. After exclusion of these cases, 23 preterm and 15 term infants remained in the study. At each center, a pediatric neuroradiologist reviewed the infants' scans, and no abnormalities were identified.

Image Processing

For each acquisition, the following image analysis steps were applied to obtain a tissue classification and a parcellation. The scans from the different centers were processed centrally by the same expert.

Because artifacts from MR field inhomogeneity pose a greater challenge in the processing of newborn brain images than in those of adults because of the reduced gray matter/white matter contrast seen in newborns, intensity nonuniformity effects, subsequent to the field inhomogeneity, were removed using a retrospective method that minimizes the entropy of the image.^{28,29} Subsequently, edge-preserving adaptive diffusion filtering³⁰ was used to reduce noise in the SPGR images while preserving subtle structures and boundaries. Rigid intra-subject registration was performed by application of an algorithm based on mutual information. The T2-weighted and proton density-weighted images were registered and upsampled to the higher resolution of the SPGR sequence.³¹

Segmentations of the ICV, cerebrospinal fluid (CSF), and 4 tissue classes (cortical gray matter [CGM], subcortical gray matter [SGM], UMWM, and MWM) were obtained using a semiautomatic segmentation method.⁹ Sample voxels were selected interactively, and optimal estimation of the distribution of MRI signal intensities associated with each type of tissue was conducted. An anatomic template was aligned with the ICV of the subject and used to disambiguate the segmentation of tissues that have overlapping signal intensity characteristics but nonoverlapping spatial distribution. Different anatomic templates were provided for the scans obtained at 32 and at 42 weeks' PMA. The sum of CGM, SGM, UMWM, and MWM defined the total volume of the cerebral parenchyma (CPAR).

The segmentation method described has been successfully applied in previous studies.^{13,14,32–34} An expert conducted 5 repeated segmentations of 5 infants' MRI scans to assess the accuracy of the segmentation approach. An algorithm called Simultaneous Truth and Performance Level Estimation (STAPLE)³⁵ was then applied to estimate for each tissue class the probability of the true segmentation of each voxel based on the repeated segmentations. The posterior probability represents the probability that a voxel truly is a particular tissue class when the segmentation states it is. The coefficient of variation of the posterior probability of the repeated segmentations was estimated to provide an indicator of the reproducibility of the method (Table 1).

The cerebellum was interactively outlined using the software package 3D Slicer³⁶ after an established and validated method.³⁴ 3D Slicer was also used to interactively align and resample all of the scans to the Talairach space.²⁵ A sagittal axis was placed through the interhemispherical fissure, and an axial axis was placed leading along the upper edge of the anterior commissure and the lower edge of the posterior commissure. Three coronal planes were placed, 1 each through the genu of the corpus callosum, the anterior, and the posterior commissure. Thus, the ICV was divided into 16 parcels (Fig 1). The coronal planes defined the partition of the ICC into 4 major regions: the frontal, precentral, central, and occipital regions.

This parcellation scheme has been demonstrated as reliable and valid for MRIs of the adult brain^{37,38} and has been applied to preterm infants' MRI.¹⁰ STAPLE³⁵ was

TABLE 1 Posterior Probability and Coefficient of Variation for Repeated Parcellations and Tissue Classification

Repeated parcellation	P1 ^a	P2	P3	P4	P5	CV
Mean PP of parcellation	0.90	0.98	0.96	0.95	0.97	4.0%
Tissue classes	CGM	SGM	UMWM	MWM	CSF	CV
Mean PP of segmentation ^b	0.84	0.80	0.90	0.80	0.89	5.4%

CV indicates coefficient of variation; PP, posterior probability.

^a Five repeated parcellations P1 to P5 were done on 1 case by the same observer.

^b Five cases were chosen for repeated segmentations, and each case was segmented 5 times by the same observer.

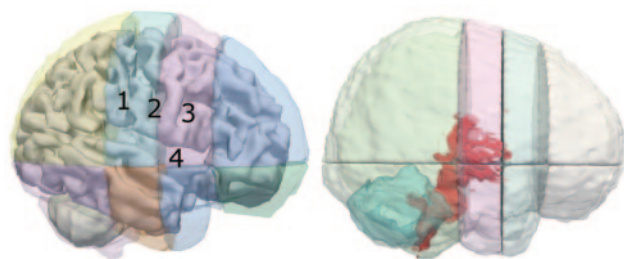


FIGURE 1

Left, Three-dimensional model of the segmented UMWM lying inside the parcellated ICV (preterm infant scanned at 32 weeks' PMA): from left to right are occipital, central, precentral, and frontal regions, each with a superior and inferior parcel. Notice the major sulci, displayed in their relation to the partitions of the parcellation: 1 indicates precentral sulcus; 2, central sulcus; 3, postcentral sulcus; 4, Sylvian fissure. Right, Three-dimensional model of the cerebellum (teal) and MWM (red) surrounded by the parcellated ICV. MWM at ~32 and 42 weeks' PMA is mainly present in the brainstem and internal capsule.

applied to assess the accuracy of the parcellation method in newborn infants in the same manner to the above described validation of the segmentation method. An expert conducted repeated parcellations of an infant's MRI scan. For each parcellation, the posterior probability of a voxel belonging to a certain parcel was computed. In addition, the coefficient of variation of the posterior probability of repeated parcellations was estimated to assess the reproducibility of the method (Table 1).

Statistical Analyses

Analysis of covariance (ANCOVA) with SPSS (SPSS Inc, Chicago, IL) was used to test for differences between tissue volumes in the scans acquired at 42 weeks' PMA in preterm versus term infants. Model testing with ICV, CPAR, and age as covariates and 2-way interactions was conducted for all of the tissue classes. Models covarying for ICV or volume of the total CPAR showed highest significance; age as a second covariate did not account significantly for variation in the model.

When Levene's test³⁹ and residual statistics showed evidence for heteroscedasticity, a heteroscedasticity-consistent SE estimator for small sample sizes, called HC3, was applied to manage heteroscedasticity of an unknown form.^{40,41} The theory and application of the HC3 method has been described elsewhere.⁴²

When testing group differences for 7 tissue classes for total and regional volumes and 16 single parcels, it is essential to correct for multiple significance tests. Benjamini and Hochberg⁴³ developed a method to control the probability of the family-wise error rate⁴⁴ by computing the false-discovery rate, which controls the expected proportion of falsely rejected hypotheses. We applied the false-discovery rate and chose a hierarchical approach to minimize the number of simultaneously tested hypotheses. Group differences for total volumes and regions were analyzed first. Only for those regions that proved to show significant differences, the right and left side and the individual parcels were subsequently

tested to further characterize the specific nature of the group differences. The number of hypotheses tested (probability level, 2-tailed: $P < .05$) was counted separately for each of the 7 segmented tissue types to allow a separate statement to be made regarding the appearance of each segmented class.

Linear regression was applied to determine absolute and relative longitudinal brain changes from 32 weeks' PMA to 42 weeks' PMA in preterm infants' serial MRI (Pearson's coefficient [r]). Regression models that correlate tissue volumes with PMA at the time of the scan and CPAR had similar significance. Reported results are based on a regression model that correlates with CPAR with the exception of the analysis of CPAR itself, which was correlated with PMA. Predicted values at 32 and 42 weeks' PMA were computed to describe total and regional rate of growth.

RESULTS

Consistency and Accuracy of the Parcellation and Segmentation Methods

For each infant's MRI study, a segmentation of the major brain tissues and a parcellation of the ICV was achieved. Through parcellation based on a limited number of landmarks, regions and parcels with consistent anatomic contents were obtained (Fig 1). At 32 and 42 weeks' PMA, the temporal lobe was located in the inferior precentral and central region and in the occipital region. The frontal region was occupied by most of the frontal lobe; a small part close to the precentral sulcus lay in the precentral region, which also included the inferior precentral gyrus. The central region contained the superior precentral gyrus and the central and postcentral gyrus. This region also enclosed the lower part of the postcentral sulcus and part of the angular gyrus. The occipital lobe and the cerebellum were included in the occipital region. Variability was seen in the association of central sulcus and precentral gyrus to the central or precentral region and the quantity of the frontal lobe that belonged to the precentral parcel (Fig 1).

A high accuracy was found for the parcellation method and the segmentation method using STAPLE³⁵ on repeated parcellations and segmentations (Table 1). Intrarater variability was low, with a coefficient of variation of 4.0% and 5.4% of the posterior probability for the parcellation and the segmentation method, respectively (Table 1).

Comparison of Brain Tissue Volumes in Term and Preterm Infants at Term: Analysis of the Relationship Among ICV, CPAR, and CSF

Twenty-three preterm infants and 15 term infants were included in the analysis. Differences in the population mean for total and regional volumes of all of the tissue classes were first tested with ICV entered as covariate.

When CSF was found to be significantly larger in preterm infants' frontal region, an analysis of head size and cerebral volume was conducted. Total and regional volumes of the ICV, CSF, and CPAR were alternately analyzed as a function of PMA at scan, ICV, and CPAR (Table 2). Total and frontal CSF and ICV were significantly larger in preterm infants when covaried with CPAR or age (Table 2). Regardless if CPAR was correlated to ICV or age, it was not different between the 2 groups. Visual inspection of a midaxial and a midsagittal slice of the infants revealed head shape differences, consistent with biparietal flattening of the skull in the preterm population. The preterm infants' heads were dolichocephalic narrow and elongated. Their frontal skull and brain appeared rounder and more prominent with a frontal accumulation of CSF, when compared with term infants (Fig 2).

When MWM was tested for possible group differences in relation to total ICV and CPAR, the volume of MWM for single parcels was significantly decreased as a fraction of the ICV but not as a fraction of the cerebral volume. This indicated the possibility for overestimation of volume differences, when normalizing with the ICV because of extraparenchymal differences between the 2 populations. Therefore, group differences between preterm and term infants were investigated in relation to the total CPAR.

Comparison of Brain Tissue Volumes at Term Correcting for CPAR

Total and regional volumes of CGM, SGM, and cerebellum did not differ significantly between preterm ($n = 23$) and term infants ($n = 15$; Table 3). Significantly increased CSF in preterm infants was found for total volume, for the frontal and precentral region, and for all 4 of the sides and all 4 of the upper parcels.

UMWM was significantly smaller in preterm infants in the central region, the right side, and the right lower parcel of the central region (Table 3). MWM was present in the central (51%) and occipital region (45%), where early appearance of myelination was confined to the brainstem, the cerebellar peduncle, and the internal capsule (Fig 1). The total volume of MWM and the volumes of the central and occipital regions were significantly smaller in preterm infants (Table 3), but none of the 4 right and left sides of both regions nor any of the 8 single

parcels reached statistical significant difference. All of the parcels, however, showed a strong trend toward significance.

In a next step, the ratio of MWM/CPAR and UMWM/CPAR was computed to express the MWM fraction and UMWM fraction of the total cerebral volume. The relation between the MWM and UMWM fractions as an indicator of WM maturation was then investigated carrying out analysis of covariance for total, central, and occipital volumes. In this analysis, the MWM fraction was expressed in relation to the UMWM fraction for preterm versus term infants. The MWM fraction was found to be significantly decreased in preterm infants ($P_{\text{total}} < .005$; $P_{\text{central}} < .005$; $P_{\text{occipital}} < .01$). This indicates a smaller ratio of MWM versus UMWM in preterm infants. Moreover, in term infants, a smaller fraction of UMWM was related to a larger fraction of MWM, but in preterm infants, for a smaller fraction of UMWM, the fraction of MWM did not increase (Fig 3). This altered correlation was found for total MWM, as well as for the volume of MWM in the central and occipital region.

Longitudinal Brain Development in Preterm Infants: Total Tissue Volumes

The serial preterm infants' scans demonstrated a steeper increase for the ICV (112%) than CPAR (103%; Table 4). Accordingly, CSF increased by 183%. Total CPAR increased from 215 to 437.6 mL between the 32 and 42 weeks' PMA, which corresponds with a daily increase in cerebral volume of 3.2 mL.

At both time points, the cerebellum was located solely in the inferior occipital region (Fig 1). It showed the largest growth rate, with a 206% increase. For all of the other tissue, CGM volume increase was largest with 167%, followed by SGM with 71%. The volume of UMWM increased by 67%, and MWM volume increased by 55% (Table 4). Pearson's coefficient for MWM (Table 4) was lower than for all of the other tissue classes ($r = 0.54$).

The composition of the cerebral tissues changed between the 2 time points at which the infants were scanned (Fig 4). At 32 weeks' PMA, the UMWM represented 57% of the CPAR. At 42 weeks' PMA, UMWM accounted only for 47% of the CPAR (49% in term infants). Average MWM remained stable, forming 2.2%

TABLE 2 Analysis of CSF, ICV, and CPAR Covaried by Age, ICV, or CPAR

Tissue Class	Preterm Infants ($n = 23$), mean \pm SD, mL	Term Infants ($n = 15$), mean \pm SD, mL	<i>P</i> (ANCOVA) Covaried by		
			PMA at Scan	Total CPAR	Total ICV
CSF total	76.4 \pm 33.9	48.9 \pm 29.9	<.02	<.02	NS
CSF frontal	21.0 \pm 10.5	9.0 \pm 6.1	<.0005	<.0005	<.001
ICV total	516.4 \pm 53.1	485.7 \pm 54.5	NS	<.02	—
ICV frontal	85.3 \pm 12.1	70.6 \pm 16.6	<.005	<.0001	—
CPAR total	440.0 \pm 35.5	436.8 \pm 42.6	NS	—	NS

NS indicates not significant.

FIGURE 2

A and B, Midsagittal MRIs; C and D, axial MRIs at the level of the anterior and posterior commissure. The parcellation of the ICV is superimposed in color. Sequence of parcels from anterior to posterior: frontal, precentral, central, and occipital parcels. A and C, a term infant's head; B and D, a preterm infant's head. Note the different head shapes; the sagittal images show a triangular-shaped frontal region in the term infant and a round shape in the preterm infant. The occipital region is elongated in the preterm infant. In the axial view, the preterm infant's head appears narrow. Anterior and posterior diameters are 113 and 125 mm; left-to-right diameter is 91 and 86 mm in the term and preterm infant, respectively.

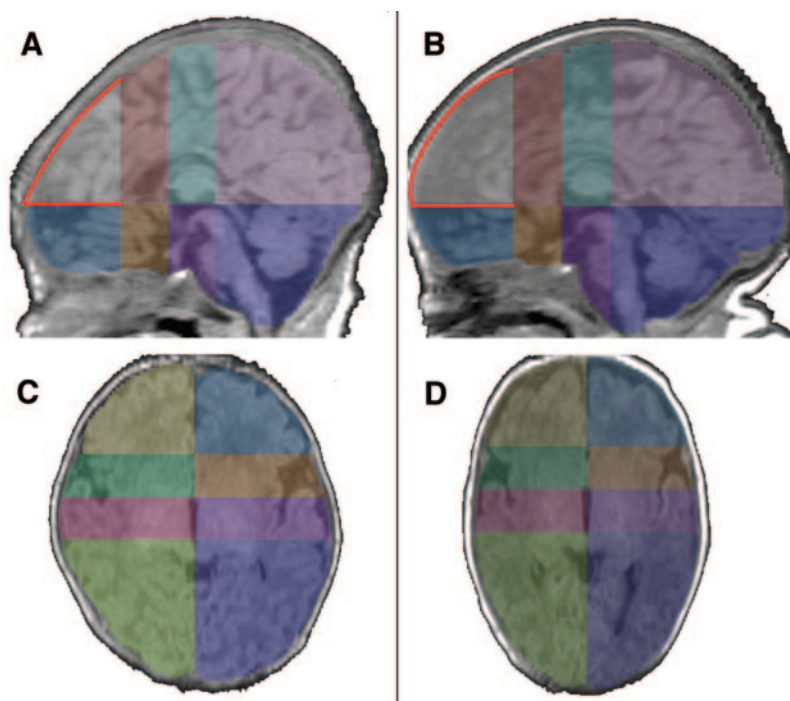


TABLE 3 Total and Significant Different Regional Brain Tissue Volumes in Preterm Versus Term Infants at 42 Weeks' PMA

Tissue Class	Preterm Infants (n = 23), Mean \pm SD, mL	Term Infants (n = 15), Mean \pm SD, mL	P (ANCOVA) ^a
CGM	176.2 \pm 26.2	162.4 \pm 23.4	NS
SGM	21.2 \pm 4.2	20.7 \pm 5.2	NS
CER	29.0 \pm 3.6	27.4 \pm 3.9	NS
UMWM	206.4 \pm 29.2	216.5 \pm 31.9	NS
Central UMWM	36.1 \pm 6.0	40.2 \pm 5.6	<.01
Right inferior central UMWM	6.8 \pm 1.1	8.0 \pm 1.1	<.0005
MWM	7.3 \pm 2.4	9.8 \pm 3.8	<.02
Central MWM	3.7 \pm 1.2	4.8 \pm 1.9	<.05
Occipital MWM	3.1 \pm 1.4	4.4 \pm 1.9	<.02

NS indicates not significant.

^a ANCOVA was carried out with CPAR as a covariate.

and 1.7% (2.1% in term infants) of total CPAR at 32 and 42 weeks' PMA, respectively. The portion of CGM increased from 30% to 39% of total CPAR between the 2 time points. The percentage of SGM of the total CPAR decreased slightly from 5.8% at 32 weeks' PMA to 4.8% at 42 weeks' PMA. At 32 weeks' PMA, the cerebellum accounted for 4.4% of the total CPAR, and at 42 weeks' PMA, the percentage was increased to 6.3% (Fig 4).

Regional Development

Volumes of all of the tissue classes in each region and Pearson's regression coefficient are reported in Table 4. In addition, it was a goal in this study to determine whether the percentage increase of the tissue volumes over time was accelerated for a certain region. Therefore, the percentage increase for each tissue in all of the

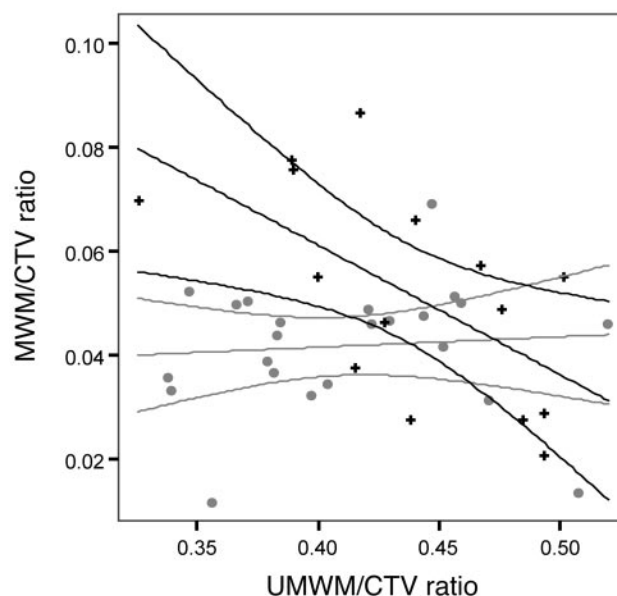


FIGURE 3

Relation between MWM and UMWM expressed as a fraction of total CPAR. +, Values for term infants; ●, values for preterm infants. Also shown are the regression line and the 95% mean prediction intervals.

regions was normalized, setting the smallest increase to 1. In this way, the ratio of the growth rate for the frontal, precentral, central, and occipital region was computed. A similar pattern for regional growth was found for ICV, CPAR, UMWM, and CGM (Table 4). The precentral and central region developed slower than the frontal and occipital region. The ICV increased faster for the frontal region, and slower for the occipital region than for all of

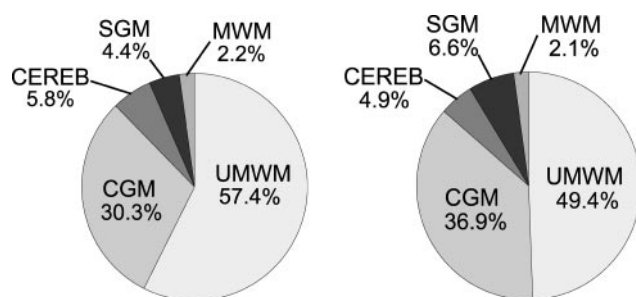
TABLE 4 Brain Tissues in Preterm Infants ($n = 23$) at 32 and 42 Weeks' PMA: Volumes and Growth Rate

Tissue Class	Frontal Region		Precentral Region		Central Region		Occipital Region		Total Brain Growth, % (r) ^b
	32 wk ^a	42 wk ^a	32 wk	42 wk	32 wk	42 wk	32 wk	42 wk	
ICV, mL	32.2	84.3	45.8	87.2	54.3	102.1	116.4	257.4	112 (0.95)
CPAR, mL	30.2	63.9	39.7	68.6	49.4	87.6	97.6	219.3	103 (0.96)
UMWM, mL	20.7	38.3	24.9	36.8	24.4	36.2	54.0	95.3	67 (0.86)
CGM, mL	9.4	25.5	11.1	25.5	16.2	36.6	28.5	86.4	167 (0.92)
SGM, mL			3.7	6.3	6.3	11.1	2.5	3.9	71 (0.70)
MWM, mL					2.4	3.7	2.0	3.1	55 (0.51)
CER, mL							9.4	28.8	206 (0.96)
Relative growth rate for each region ^c									
ICV	1.8	:	1.0	:	1.0	:	1.4		
CPAR	1.5	:	1.0	:	1.0	:	1.6		
UMWM	1.8	:	1.0	:	1.0	:	1.6		
CGM	1.3	:	1.0	:	1.0	:	1.6		
SGM			1.2	:	1.3	:	1.0		
MWM					1.0	:	1.0		

^a Predicted tissue volumes at 32 and 42 weeks' PMA in relation to PMA at scan.

^b Regression coefficient r with PMA at scan as dependent variable is given for total tissue development.

^c Growth rate reveals the region of fastest growth.

**FIGURE 4**

Composition of cerebral tissue volume by its single components at 32 weeks' PMA (left) and 42 weeks' PMA (right).

the other brain tissues tested. CGM showed a slower growth rate in the frontal region as compared with the UMWM and CPAR. At both time points, growth rate for MWM was similar for the central and occipital region. No MWM was found in the frontal and precentral region. SGM was found to grow more slowly in the occipital than in the central region. It was not detected in the frontal and precentral region at either of the time points.

DISCUSSION

Comparison of Preterm and Term Infants' Brain Tissue Volumes

Effects of Premature Birth on Intracranial, Cerebral, and CSF Volumes

Studies have shown head circumference to be a reliable indicator of an infant's gestational age if the infants' growth is appropriate for its gestational age.^{45,46} Hence, most newborn infant studies that involve tissue classification have used intracranial volume as an indicator for the infant's head size and expressed brain tissue volumes relative to intracranial volume.^{11,13,14,33,47} This approach assumes that head growth progresses in a similar fashion

after preterm and term birth and that cerebral growth influences head size and shape similarly in both populations.

However, in the current study, gross assessment of the infants' MRI revealed biparietal narrowed and fronto-occipital elongated heads in the preterm population accompanied by regionally increased CSF volumes. Biparietal flattening occurs in response to external compression force exerted during sleep position in incubators and cribs⁴⁸ during the first days after preterm birth.^{49–51} Mode of delivery does not implicate flattening of the skull.⁵² In normal infants, head circumference as assessed in ultrasound biometry serves as a good indicator for brain size. However, if the head shape is abnormal and head growth is accelerated, this is not the case.^{53,54} Thus, other measures are suggested for preterm infants, such as the cerebellar diameter, which reliably measures adequate growth even when the infant exhibits an unusually shaped head.^{55,56}

Studies using MRI biomarkers such as tissue volumes are sparse. Duncan et al⁵⁷ found head circumference measured in fetal imaging to be a poor indicator for brain size in infants with fetal growth restriction. Several investigations in preterm infants with brain injury have identified an association between increased CSF volumes and decreased cerebral volumes.^{11,13,47} The current study provides the first evidence to suggest that, in low-risk preterm infants, those selected to have a head circumference appropriate for their PMA, cerebral volume is normal, yet CSF volume is increased. Considering that an appropriate head circumference between the 10th and 90th percentile corresponds with 33- to 38-cm head circumference measured at birth, this gives a broad range of variable brain tissue and CSF volumes, which may obscure true group differences in a small cohort. Results from the longitudinal analysis, which show a

distinct growth pattern for the CSF volume and the slower increasing cerebral volume, support the findings of the comparison between preterm and term infants. Future work is needed to investigate the association between changes in preterm infants' head shape and tissue volumes and to identify the effect that this might have on the reliability of a landmark-based parcellation.

Effects of Premature Birth on Gray Matter Volumes

Quantitative MRI studies, which investigated preterm infants with white matter injury, those born very early, and those with fetal growth restriction, have found decreased gray matter volumes in preterm infants.^{14,32,47} These changes have been further associated with impaired neurodevelopmental outcome.³² During late gestation, after the migration of neurons into the cortex is completed, decreased gray matter volumes may be caused by atrophy and neuronal loss, disruption of the formation of neural connectivity and of dendrite growth during synaptogenesis.^{58–60} The undisturbed gray matter development found in the preterm sample of the current study might explain the only moderate neurodevelopmental differences otherwise reported in low-risk AGA preterm infants.^{23,24,61}

Effects of Premature Birth on Total and Regional White Matter Volumes

Although statistical analyses identified significant differences of regional white matter volumes between preterm and term infants, testing of single parcels failed to reach statistical significance. This underlines the importance of regional assessment when investigating brain development but also points to the limitations of measuring regional and therewith often very small volumes.

Reduction in statistical power makes interpretation of such results difficult, especially given the relatively small sample of the current study, which consisted of 23 preterm and 15 term infants after exclusion of 5 infants because of motion artifacts. An alternative definition of parcels may also improve sensitivity to differences in myelination, because myelination follows an anatomically specific developmental process.⁶²

Similar to the current study, Peterson et al⁴⁷ reported findings of decreased white matter in the central region, which includes the sensor-motor system, as well as the auditory processing areas of the frontotemporal lobes. In addition, the preterm infants in that study displayed decreased white matter volumes in the parieto-occipital regions when compared with term infants. A possible explanation for the differences between the results of Peterson et al⁴⁷ and the current study is the fact that the preterm infants in the study by Peterson et al⁴⁷ experienced several clinical complications, such as periventricular leukomalacia and bronchopulmonary dysplasia treated with postnatal steroids, which are known to affect brain development. It is likely that, therefore, the

preterm brains in the study by Peterson et al⁴⁷ were impaired to a more extended degree.

The current study suggests an alteration in the course of myelination for the preterm infants studied. In these infants, a decrease of UMWM fraction was not always accompanied by an increase in the myelinated fraction. Whether these observations are caused by unidentified injury, delay, or an alteration of fiber tract development cannot be answered with the present study. New techniques, such as the analysis of diffusion tensor imaging, have been applied recently to preterm and term MRI.⁶³ Initial findings show promising results for the analysis of white matter maturation. Evidence has been found recently for underlying delay in white matter maturation in preterm infants with brain injury,^{64,65} as well as in AGA preterm infants without brain injury.²⁶

Longitudinal Brain Development in Preterm Infants

Growth of Total Cerebral Tissues

Literature on fetal biometry was reviewed to compare postnatal measures from this study to reference values from fetal imaging. Fetal MRI and ultrasound^{66–69} have been used to estimate fetal brain volumes in normal pregnancies, and best-fit regression equations have been reported. Postprocessing methods range from estimation of brain volume to an exact labeling of the boundaries in each slice to outline the brain.⁶⁸ Daily increase in cerebral tissue volume has been reported in a number of publications^{66–69} with a range of 2.3 to 3.6 mL and a mean of 3.1 mL. Whereas the current study's methods were not directly comparable, because postprocessing methodology differed, daily growth rate was similar with 3.2 mL per day. This should be encouraging for future investigations, which may use data from low-risk uncomplicated preterm infants as a model for the investigation of brain development.

Single Brain Tissue Development and Tissue Composition of the Brain

Longitudinal analysis of the brain tissue composition suggested that the developmental period studied seems to be a critical period for cerebral gray matter growth. One possible explanation is that because neural migration itself gradually ends by the beginning of the third trimester, the pronounced increase in gray matter volume may indicate the increasingly rich axonal branching and developing connectivity between neurons, as well as synaptogenesis.^{70–72} CGM volume is further influenced by cortical folding, which increases markedly during the studied period between 32 and 40 weeks. Cortical folding is more prominent in the occipital lobe than in the frontal lobe, which is reflected in the higher growth rate for CGM volume in the occipital lobe than in the frontal lobe.

Another consideration is that cortical thickness as measured by MRI is influenced by tissue characteristics,

such as water content. During cortical development, inner layers of the cortex have higher water content, which might lead to a falsely thin cortical rim on MRI and, consequently, to an underestimation of the cortical volume by the proposed segmentation techniques. Myelination leads to decreased water content followed by signal intensity changes of the white matter and the adjacent gray matter. The rapid gray matter volume change in the preterm infants' cortex observed in the current study might, thus, be related to a physiologic decrease in the water content during ongoing white matter maturation,¹⁷ leading to an overestimation of the increase in gray matter volume.

CONCLUSIONS

This study provides evidence that low-risk AGA preterm infants show moderate regional differences for white matter development in comparison with healthy term infants. In contrast, the regional pattern for gray matter development was not affected in the studied preterm population. These findings are consistent with studies reporting moderate neurodevelopmental delay in low-risk preterm infants. Longitudinal analysis of preterm infants' serial data demonstrated that the brain tissue composition changes from 32 to 42 weeks' PMA, presenting a decreasing partition of UMWM in favor of gray matter growth and an accentuated growth of the frontal and occipital region.

ACKNOWLEDGMENTS

This study was supported in part by the Whitaker Foundation; National Institutes of Health grants R01 HD38261, R21 MH67054, R01 LM007861, P41 RR13218, and P30 HD18655; US Department of Education grants H023C70032 and R305T990294; and Swiss National Foundation grants SNF 32-56927.99 and 3200-102127.

We acknowledge the time and efforts of the Murdoch Childrens Research Institute of Melbourne, Australia, affiliated with Dr Inder, in helping to achieve the MR acquisitions and Joao Fernandes in helping to achieve segmentations of the infants' MRI scans.

REFERENCES

- Hack M, Taylor HG. Perinatal brain injury in preterm infants and later neurobehavioral function. *JAMA*. 2000;284:1973-1974
- Marlow N, Wolke D, Bracewell MA, Samara M. Neurologic and developmental disability at six years of age after extremely preterm birth. *N Engl J Med*. 2005;352:9-19
- O'Shea TM, Counsell SJ, Bartels DB, Dammann O. Magnetic resonance and ultrasound brain imaging in preterm infants. *Early Hum Dev*. 2005;81:263-271
- Huppi PS, Amato M. Advanced magnetic resonance imaging techniques in perinatal brain injury. *Biol Neonate*. 2001;80:7-14
- Volpe JJ. Perinatal brain injury: from pathogenesis to neuroprotection. *Ment Retard Dev Disabil Res Rev*. 2001;7:56-64
- Kendall G, Peebles D. Acute fetal hypoxia: the modulating effect of infection. *Early Hum Dev*. 2005;81:27-34
- Graham EM, Holcroft CJ, Rai KK, Donohue PK, Allen MC. Neonatal cerebral white matter injury in preterm infants is associated with culture positive infections and only rarely with metabolic acidosis. *Am J Obstet Gynecol*. 2004;191:1305-1310
- Inder TE, Wells SJ, Mogridge NB, Spencer C, Volpe JJ. Defining the nature of the cerebral abnormalities in the premature infant: a qualitative magnetic resonance imaging study. *J Pediatr*. 2003;143:171-179
- Warfield SK, Kaus M, Jolesz FA, Kikinis R. Adaptive, template moderated, spatially varying statistical classification. *Med Image Anal*. 2000;4:43-55
- Peterson BS, Vohr B, Staib LH, et al. Regional brain volume abnormalities and long-term cognitive outcome in preterm infants. *JAMA*. 2000;284:1939-1947
- Inder TE, Huppi PS, Warfield S, et al. Periventricular white matter injury in the premature infant is followed by reduced cerebral cortical gray matter volume at term. *Ann Neurol*. 1999;46:755-760
- Toft PB, Leth H, Ring PB, Peitersen B, Lou HC, Henriksen O. Volumetric analysis of the normal infant brain and in intrauterine growth retardation. *Early Hum Dev*. 1995;43:15-29
- Tolsa CB, Zimine S, Warfield SK, et al. Early alteration of structural and functional brain development in premature infants born with intrauterine growth restriction. *Pediatr Res*. 2004;56:132-138
- Murphy BP, Inder TE, Huppi PS, et al. Impaired cerebral cortical gray matter growth after treatment with dexamethasone for neonatal chronic lung disease. *Pediatrics*. 2001;107:217-221
- Abernethy LJ, Palaniappan M, Cooke RW. Quantitative magnetic resonance imaging of the brain in survivors of very low birth weight. *Arch Dis Child*. 2002;87:279-283
- Kesler SR, Ment LR, Vohr B, et al. Volumetric analysis of regional cerebral development in preterm children. *Pediatr Neurol*. 2004;31:318-325
- Counsell SJ, Maalouf EF, Fletcher AM, et al. MR imaging assessment of myelination in the very preterm brain. *AJNR Am J Neuroradiol*. 2002;23:872-881
- Huppi PS, Warfield S, Kikinis R, et al. Quantitative magnetic resonance imaging of brain development in premature and mature newborns. *Ann Neurol*. 1998;43:224-235
- Martin JA, Hamilton BE, Sutton PD, Ventura SJ, Menacker F, Munson ML. Births: final data for 2002. *Natl Vital Stat Rep*. 2003;52(10):1-113
- Martin JA, Hamilton BE, Ventura SJ, Menacker F, Park MM, Sutton PD. Births: final data for 2001. *Natl Vital Stat Rep*. 2002;51(2):1-102
- Hemgren E, Persson K. Quality of motor performance in preterm and full-term 3-year-old children. *Child Care Health Dev*. 2004;30:515-527
- Vollmer B, Roth S, Baudin J, Stewart AL, Neville BG, Wyatt JS. Predictors of long-term outcome in very preterm infants: gestational age versus neonatal cranial ultrasound. *Pediatrics*. 2003;112:1108-1114
- Pietz J, Peter J, Graf R, et al. Physical growth and neurodevelopmental outcome of nonhandicapped low-risk children born preterm. *Early Hum Dev*. 2004;79:131-143
- Gutbrod T, Wolke D, Soehne B, Ohrt B, Riegel K. Effects of gestation and birth weight on the growth and development of very low birthweight small for gestational age infants: a matched group comparison. *Arch Dis Child Fetal Neonatal Ed*. 2000;82:F208-F214
- Talairach JTP. *Co-Planar Stereotaxic Atlas of the Human Brain*. New York, NY: Thieme Medical Publishers; 1988
- Als H, Duffy FH, McAnulty GB, et al. Early experience alters brain function and structure. *Pediatrics*. 2004;113:846-857

27. Engle WA. Age terminology during the perinatal period. *Pediatrics*. 2004;114:1362–1364
28. Weisenfeld NL, Warfield SK. Normalization of joint image-intensity statistics in MRI using the Kullback-Leibler divergence. Presented at: ISBI 2004 2nd IEEE International Symposium on Biomedical Imaging: From Nano to Macro; April 15–18, 2004; Arlington, VA
29. Mangin J. Entropy minimization for automatic correction of intensity non-uniformity. Presented at: Mathematical Methods in Biomedical Image Analysis; June 11–12, 2000; Hilton Head Island, SC
30. Krissian K. Flux-based anisotropic diffusion applied to enhancement of 3-D angiogram. *IEEE Trans Med Imaging*. 2002;21:1440–1442
31. Wells WM 3rd, Viola P, Atsumi H, Nakajima S, Kikinis R. Multi-modal volume registration by maximization of mutual information. *Med Image Anal*. 1996;1:35–51
32. Inder TE, Warfield SK, Wang H, Huppi PS, Volpe JJ. Abnormal cerebral structure is present at term in premature infants. *Pediatrics*. 2005;115:286–294
33. Hunt RW, Warfield SK, Wang H, Kean M, Volpe JJ, Inder TE. Assessment of the impact of the removal of cerebrospinal fluid on cerebral tissue volumes by advanced volumetric 3D-MRI in posthaemorrhagic hydrocephalus in a premature infant. *J Neurol Neurosurg Psychiatry*. 2003;74:658–660
34. Limperopoulos C, Soul JS, Gauvreau K, et al. Late gestation cerebellar growth is rapid and impeded by premature birth. *Pediatrics*. 2005;115:688–695
35. Warfield SK, Zou KH, Wells WM. Simultaneous truth and performance level estimation (STAPLE): an algorithm for the validation of image segmentation. *IEEE Trans Med Imaging*. 2004;23:903–921
36. Gering DT, Nabavi A, Kikinis R, et al. An integrated visualization system for surgical planning and guidance using image fusion and an open MRI. *J Magn Reson Imaging*. 2001;13:967–975
37. Makris N, Meyer JW, Bates JF, Yeterian EH, Kennedy DN, Caviness VS. MRI-Based topographic parcellation of human cerebral white matter and nuclei II. Rationale and applications with systematics of cerebral connectivity. *Neuroimage*. 1999;9:18–45
38. Meyer JW, Makris N, Bates JF, Caviness VS, Kennedy DN. MRI-Based topographic parcellation of human cerebral white matter. *Neuroimage*. 1999;9:1–17
39. Levene H. Essays in honor of Harold Hotelling. *Contrib Prob Stat*. 1960:278–292
40. MacKinnon J, White H. Some heteroscedasticity-consistent covariance matrix estimators with improved finite sample properties. *J Econom*. 1985;29:305–325
41. Long J, Ervin L, Laurie H. Using heteroscedasticity consistent standard errors in the linear regression model. *Am Stat*. 2000;54:217–224
42. Hayes AF. *Statistical Methods for Communication Science*. 1st ed. Mahwah, NJ: Lawrence Erlbaum Associates; 2005
43. Benjamini Y, Hochberg Y. Controlling the false discovery rate: a practical and powerful approach to multiple testing. *J R Stat Soc Ser B*. 1995;57:289–300
44. Hochberg Y, Tamhane A. *Multiple Comparison Procedures*. New York, NY: Wiley; 1987
45. Dobbing J, Sands J. Quantitative growth and development of human brain. *Arch Dis Child*. 1973;48:757–767
46. Guihard-Costa AM, Menez F, Delezoide AL. Organ weights in human fetuses after formalin fixation: standards by gestational age and body weight. *Pediatr Dev Pathol*. 2002;5:559–578
47. Peterson BS, Anderson AW, Ehrenkranz R, et al. Regional brain volumes and their later neurodevelopmental correlates in term and preterm infants. *Pediatrics*. 2003;111:939–948
48. Hutchison BL, Hutchison LA, Thompson JM, Mitchell EA. Plagiocephaly and brachycephaly in the first two years of life: a prospective cohort study. *Pediatrics*. 2004;114:970–980
49. Hutchison BL, Thompson JM, Mitchell EA. Determinants of nonsynostotic plagiocephaly: a case-control study. *Pediatrics*. 2003;112(4). Available at: www.pediatrics.org/cgi/content/full/112/4/e316
50. Carlan SJ, Wyble L, Lense J, Mastrogianis DS, Parsons MT. Fetal head molding. Diagnosis by ultrasound and a review of the literature. *J Perinatol*. 1991;11:105–111
51. Huang MH, Mouradian WE, Cohen SR, Gruss JS. The differential diagnosis of abnormal head shapes: separating craniosynostosis from positional deformities and normal variants. *Cleft Palate Craniofac J*. 1998;35:204–211
52. Souza SW, Ross J, Milner RD. Alterations in head shape of newborn infants after caesarean section or vaginal delivery. *Arch Dis Child*. 1976;51:624–627
53. Buda FB, Reed JC, Rabe EF. Skull volume in infants. Methodology, normal values, and application. *Am J Dis Child*. 1975;129:1171–1174
54. Houlton MC, Brennan DT. Dolichocephaly—a source of error in serial cephalometry. *Br J Obstet Gynaecol*. 1976;83:276–278
55. Cabbad M, Kofinas A, Simon N, King K, Lytle E. Fetal weight-cerebellar diameter discordance as an indicator of asymmetrical fetal growth impairment. *J Reprod Med*. 1992;37:794–798
56. Goldstein I, Reece EA, Pilu G, Bovicelli L, Hobbins JC. Cerebellar measurements with ultrasonography in the evaluation of fetal growth and development. *Am J Obstet Gynecol*. 1987;156:1065–1069
57. Duncan KR, Issa B, Moore R, Baker PN, Johnson IR, Gowland PA. A comparison of fetal organ measurements by echo-planar magnetic resonance imaging and ultrasound. *BJOG*. 2005;112:43–49
58. Marin-Padilla M. Prenatal development of fibrous (white matter), protoplasmic (gray matter), and layer I astrocytes in the human cerebral cortex: a Golgi study. *J Comp Neurol*. 1995;357:554–572
59. Marin-Padilla M. Developmental neuropathology and impact of perinatal brain damage. I: Hemorrhagic lesions of neocortex. *J Neuropathol Exp Neurol*. 1996;55:758–773
60. Marin-Padilla M. Developmental neuropathology and impact of perinatal brain damage. II: white matter lesions of the neocortex. *J Neuropathol Exp Neurol*. 1997;56:219–235
61. Duffy FH, Als H, McNulty GB. Behavioral and electrophysiological evidence for gestational age effects in healthy preterm and fullterm infants studied two weeks after expected due date. *Child Dev*. 1990;61:271–286
62. Kinney HC, Brody BA, Kloman AS, Gilles FH. Sequence of central nervous system myelination in human infancy. II. Patterns of myelination in autopsied infants. *J Neuropathol Exp Neurol*. 1988;47:217–234
63. Huppi PS, Maier SE, Peled S, et al. Microstructural development of human newborn cerebral white matter assessed in vivo by diffusion tensor magnetic resonance imaging. *Pediatr Res*. 1998;44:584–590
64. Miller SP, Vigneron DB, Henry RG, et al. Serial quantitative diffusion tensor MRI of the premature brain: development in newborns with and without injury. *J Magn Reson Imaging*. 2002;16:621–632
65. Huppi PS, Murphy B, Maier SE, et al. Microstructural brain development after perinatal cerebral white matter injury assessed by diffusion tensor magnetic resonance imaging. *Pediatrics*. 2001;107:455–460
66. Duncan KR, Sahota DS, Gowland PA, et al. Multilevel modeling of fetal and placental growth using echo-planar magnetic resonance imaging. *J Soc Gynecol Investig*. 2001;8:285–290
67. Gong QY, Roberts N, Garden AS, Whitehouse GH. Fetal and fetal brain volume estimation in the third trimester of human

- pregnancy using gradient echo MR imaging. *Magn Reson Imaging*. 1998;16:235–240
68. Roelfsema NM, Hop WC, Boito SM, Wladimiroff JW. Three-dimensional sonographic measurement of normal fetal brain volume during the second half of pregnancy. *Am J Obstet Gynecol*. 2004;190:275–280
 69. Chang CH, Yu CH, Chang FM, Ko HC, Chen HY. The assessment of normal fetal brain volume by 3-D ultrasound. *Ultrasound Med Biol*. 2003;29:1267–1272
 70. Huttenlocher PR, Dabholkar AS. Regional differences in synaptogenesis in human cerebral cortex. *J Comp Neurol*. 1997;387:167–178
 71. Bourgeois JP, Goldman-Rakic PS, Rakic P. Synaptogenesis in the prefrontal cortex of rhesus monkeys. *Cereb Cortex*. 1994;4:78–96
 72. Rakic P, Bourgeois JP, Eckenhoﬀ MF, Zecevic N, Goldman-Rakic PS. Concurrent overproduction of synapses in diverse regions of the primate cerebral cortex. *Science*. 1986;232:232–235

THE BAND-AID

“But when Earle Dickson invented the adhesive bandage in 1920, he saw it as an ingenious and effective solution to a serious problem. In doing so, he created an immensely useful product as well as a universally recognized brand. Dickson was a cotton buyer for Johnson & Johnson. According to Lawrence G. Foster, who helped launch the company’s public relations department in the 1950’s and later served as its unofficial historian, Dickson’s wife, Josephine, was ‘not very adept in the kitchen.’ Company lore has it that she was forever suffering minor cuts and burns while cooking. Applying cotton gauze and surgical tape proved difficult to do one-handed, so she often summoned her husband home to help. Johnson & Johnson had been making sterile dressings and adhesive surgical tapes for decades. Dickson simply put the two together in a single convenient package. He affixed squares of cotton gauze to a long strip of tape and covered the whole thing with crinoline, which would prevent the tape from sticking to itself when rolled up and keep the gauze reasonably aseptic. Mrs. Dickson could cut off a piece from the strip, peel off the crinoline, and bandage her wound. Dickson described his invention to a coworker, who encouraged him to tell his boss about it. ‘The boys in the front office loved the concept,’ Dickson said years later. The general public was not as enthusiastic. In the first year, sales were a disappointing \$3,000. But the first Band-Aids, which were handmade, measured 2½ inches wide and 18 inches long, so they couldn’t have been an enormous breakthrough in convenience. The advertising firm of Young and Rubicam told the company that they were a lost cause, but Johnson & Johnson kept faith in the product. Automated manufacturing, more convenient packaging, and aggressive marketing eventually helped turn Band-Aids into one of the most successful consumer products in history, with more than 100 billion sold over the last 80 years. . . . History hasn’t recorded the fate of Josephine Dickson, but her husband was well rewarded for his innovation, becoming a vice president at Johnson & Johnson and later a member of the company’s board of directors, so perhaps if those stories were actually true, he was able to hire his wife a cook.”

Wohleber C. *Invention & Technology*. Summer 2005

Noted by JFL, MD

Regional Brain Development in Serial Magnetic Resonance Imaging of Low-Risk Preterm Infants

Andrea U.J. Mewes, Petra S. Hüppi, Heidelise Als, Frank J. Rybicki, Terrie E. Inder, Gloria B. McAnulty, Robert V. Mulkern, Richard L. Robertson, Michael J. Rivkin and Simon K. Warfield

Pediatrics 2006;118;23

DOI: 10.1542/peds.2005-2675

Updated Information & Services	including high resolution figures, can be found at: http://pediatrics.aappublications.org/content/118/1/23.full.html
References	This article cites 62 articles, 18 of which can be accessed free at: http://pediatrics.aappublications.org/content/118/1/23.full.html#ref-list-1
Citations	This article has been cited by 7 HighWire-hosted articles: http://pediatrics.aappublications.org/content/118/1/23.full.html#related-urls
Subspecialty Collections	This article, along with others on similar topics, appears in the following collection(s): Fetus/Newborn Infant http://pediatrics.aappublications.org/cgi/collection/fetus:newborn_infant_sub Neonatology http://pediatrics.aappublications.org/cgi/collection/neonatology_sub Neurology http://pediatrics.aappublications.org/cgi/collection/neurology_sub Radiology http://pediatrics.aappublications.org/cgi/collection/radiology_sub
Permissions & Licensing	Information about reproducing this article in parts (figures, tables) or in its entirety can be found online at: http://pediatrics.aappublications.org/site/misc/Permissions.xhtml
Reprints	Information about ordering reprints can be found online: http://pediatrics.aappublications.org/site/misc/reprints.xhtml

PEDIATRICS is the official journal of the American Academy of Pediatrics. A monthly publication, it has been published continuously since 1948. PEDIATRICS is owned, published, and trademarked by the American Academy of Pediatrics, 141 Northwest Point Boulevard, Elk Grove Village, Illinois, 60007. Copyright © 2006 by the American Academy of Pediatrics. All rights reserved. Print ISSN: 0031-4005. Online ISSN: 1098-4275.

American Academy of Pediatrics

DEDICATED TO THE HEALTH OF ALL CHILDREN™



PEDIATRICS®

OFFICIAL JOURNAL OF THE AMERICAN ACADEMY OF PEDIATRICS

Regional Brain Development in Serial Magnetic Resonance Imaging of Low-Risk Preterm Infants

Andrea U.J. Mewes, Petra S. Hüppi, Heidelise Als, Frank J. Rybicki, Terrie E. Inder, Gloria B. McAnulty, Robert V. Mulkern, Richard L. Robertson, Michael J. Rivkin and Simon K. Warfield

Pediatrics 2006;118;23

DOI: 10.1542/peds.2005-2675

The online version of this article, along with updated information and services, is located on the World Wide Web at:

<http://pediatrics.aappublications.org/content/118/1/23.full.html>

PEDIATRICS is the official journal of the American Academy of Pediatrics. A monthly publication, it has been published continuously since 1948. PEDIATRICS is owned, published, and trademarked by the American Academy of Pediatrics, 141 Northwest Point Boulevard, Elk Grove Village, Illinois, 60007. Copyright © 2006 by the American Academy of Pediatrics. All rights reserved. Print ISSN: 0031-4005. Online ISSN: 1098-4275.

American Academy of Pediatrics

DEDICATED TO THE HEALTH OF ALL CHILDREN™

